Journal of Nuclear Medicine, published on November 9, 2012 as doi:10.2967/jnumed.112.104588

Altered $GABA_A$ Receptor Density and Unaltered Blood–Brain Barrier Transport in a Kainate Model of Epilepsy: An In Vivo Study Using ^{11}C-Flumazenil and PET

Stina Syvänen[1], Maaike Labots[1], Yoshihiko Tagawa[2], Jonas Eriksson[3], Albert D. Windhorst[3], Adriaan A. Lammertsma[3], Elizabeth C. de Lange[1], and Rob A. Voskuyl[1,4]

[1]Division of Pharmacology, LACDR, Leiden University, Leiden, The Netherlands; [2]Takeda Chemical Industries Ltd., Yodogawa-ku, Osaka, Japan; [3]Department of Nuclear Medicine and PET Research, VU University Medical Center, Amsterdam, The Netherlands; and [4]SEIN–Epilepsy Institutes of The Netherlands Foundation, Heemstede, The Netherlands

The aim of the present study was to investigate if flumazenil blood–brain barrier transport and binding to the benzodiazepine site on the γ-aminobutyric acid A ($GABA_A$) receptor complex is altered in an experimental model of epilepsy and subsequently to study if changes in P-glycoprotein (P-gp)–mediated efflux of flumazenil at the blood–brain barrier may confound interpretation of ^{11}C-flumazenil PET in epilepsy. **Methods:** The transport of flumazenil across the blood–brain barrier and the binding to the benzodiazepine site on the $GABA_A$ receptors in 5 different brain regions was studied and compared between controls and kainate-treated rats, a model of temporal lobe epilepsy, with and without tariquidar pretreatment. In total, 29 rats underwent 2 consecutive ^{11}C-flumazenil PET scans, each one lasting 30 min. The tracer was mixed with different amounts of isotopically unmodified flumazenil (4, 20, 100, or 400 μg) to cover a wide range of receptor occupancies during the scan. Before the second scan, the rats were pretreated with a 3 or 15 mg/kg dose of the P-gp inhibitor tariquidar. The second scan was then obtained according to the same protocol as the first scan. **Results:** $GABA_A$ receptor density, B_{max}, was estimated as 44 ± 2 ng·mL^{-1} in the hippocampus and as 33 ± 2 ng·mL^{-1} in the cerebellum, with intermediate values in the occipital cortex, parietal cortex, and caudate putamen. B_{max} was decreased by 12% in kainate-treated rats, compared with controls. The radiotracer equilibrium dissociation constant, K_D, was similar in both rat groups and all brain regions and was estimated as 5.9 ± 0.9 ng·mL^{-1}. There was no difference in flumazenil transport across the blood–brain barrier between control and kainate-treated rats, and the effect of tariquidar treatment was similar in both rat groups. Tariquidar treatment also decreased flumazenil transport out of the brain by 73%, increased the volume of distribution in the brain by 24%, and did not influence B_{max} or K_D, compared with baseline. **Conclusion:** B_{max} was decreased in kainate-treated rats, compared with controls, but no alteration in the blood–brain barrier transport of flumazenil was observed. P-gp inhibition by tariquidar treatment increased brain concentrations of flumazenil in both groups, but B_{max} estimates were not influenced, suggesting that ^{11}C-flumazenil scanning is not confounded by alterations in P-gp function.

Key Words: positron emission tomography; $GABA_A$ receptors; P-glycoprotein; pharmacokinetics; epilepsy

J Nucl Med 2012; 53:1–10
DOI: 10.2967/jnumed.112.104588

There is overwhelming evidence from preclinical and clinical studies that γ-aminobutyric acid (GABA), the chief inhibitory neurotransmitter in the mammalian central nervous system, has an important role in epilepsy. Drugs that antagonize $GABA_A$ receptor activation invariably cause seizures (*1,2*), and several efficacious antiepileptic drugs act by enhancing $GABA_A$-mediated inhibition (*3–6*).

$GABA_A$ receptor properties and binding of ligands (drugs) to the benzodiazepine site on the receptor can be studied in vivo using PET and ^{11}C-labeled flumazenil. ^{11}C-flumazenil binds to the benzodiazepine site on the $GABA_A$ receptor complex. The binding kinetics of ^{11}C-flumazenil to $GABA_A$ receptors are dependent on receptor density (B_{max}) and affinity of flumazenil for the receptor (K_D). The decreased efficacy of GABAergic drugs observed in people with drug-resistant epilepsy could be attributed to alterations in B_{max} or altered substrate binding affinity K_D. Evidence suggesting that flumazenil is a P-glycoprotein (P-gp) substrate has recently emerged (*7*). It has been hypothesized that P-gp function is upregulated in epilepsy and, further, that an upregulation in P-gp could alter transport of ^{11}C-flumazenil into the brain and binding to $GABA_A$ receptors in epilepsy. Increased P-gp action may also, at least in part, be responsible for pharmacoresistance by impairing drug access to the brain in people with severe epilepsy (*8,9*). Thus, the present study aimed at investigating the hypothesis that $GABA_A$ receptor or P-gp function is altered in epilepsy.

The kainate model in rats displays several features of temporal lobe epilepsy, the form of epilepsy that is most

Received Feb. 17, 2012; revision accepted Jul. 24, 2012.
For correspondence or reprints contact: Stina Syvänen, Division of Pharmacology, LACDR, P.O. Box 9502, 2300 RA Leiden, The Netherlands.
E-mail: s.syvanen@lacdr.leidenuniv.nl
Published online ■■■■.

frequently associated with pharmacoresistance; therefore, this model was chosen for the present study. The objectives were to compare flumazenil brain pharmacokinetics—that is, transport across the blood–brain barrier and binding within the brain—between control rats and kainate-treated rats, to assess whether flumazenil pharmacokinetics can be modulated by the P-gp inhibitor tariquidar, and to determine whether this modulation differs between control and kainate-treated animals.

MATERIALS AND METHODS

Animals

Thirty-two adult male Sprague–Dawley rats (Harlan), weighing 200–224 g on arrival, were housed in groups of 5–6 per cage. They were kept at a constant temperature of 21°C and kept on a 12-h light–dark cycle, in which lights were switched on at 8 AM. Animals had unrestricted access to food (Teklad Global 16% Protein Rodent Diet; Harlan) and water. Animal procedures were performed in accordance with Dutch laws on animal experimentation. All experiments were approved by the Ethics Committee for Animal Experiments of Leiden University (approval nos. UDEC08179 and UDEC09194). After approximately 1 wk of habituation, 17 rats were treated with kainic acid until full-blown seizures were observed (*10*). An initial dose of 10 $mg \cdot kg^{-1}$ (2 $mL \cdot kg^{-1}$) was administered by intraperitoneal injection, followed by 5 $mg \cdot kg^{-1}$ (1 $mL \cdot kg^{-1}$) every 30–60 min until the animal had stage IV seizures according to the scale of Racine et al. (*11*) or when a total amount of 30 $mg \cdot kg^{-1}$ of kainic acid had been reached. All animals developed status epilepticus within 20 min after the last injection. Rats usually experienced seizures for 6–12 h, with the most intense and frequent seizures occurring during the first 2 h. Rats underwent PET at 7 ($n = 12$) or 2 ($n = 3$) days after kainate treatment. Control animals ($n = 14$) underwent PET after at least 1 wk of habituation. Two animals died as a consequence of the kainate treatment, and 1 control rat died during surgery before the PET experiments.

Radiochemistry

^{11}C-flumazenil was synthesized as previously described (*12*), yielding 3–8 GBq formulated in 10 mL of buffered saline (7.1 mM NaH_2PO_4) containing 10% ethanol. Specific activity was 172 ± 58 (mean ± SD) $GBq \cdot \mu mol^{-1}$ at the end of synthesis. Radiochemical purity was greater than 99%, and no chemical impurities were observed as assessed by radio–high-performance liquid chromatography or ultraviolet high-performance liquid chromatography.

PET Experiments

Anesthesia was induced by intraperitoneal injection of a 60 $mg \cdot kg^{-1}$ dose of ketamine (Ketalar; Parke-Davis) and a 0.4 $mg \cdot kg^{-1}$ dose of medetomidine (Domitor; Pfizer), followed 60 min later by an infusion into the tail vein of a 10 $mg \cdot kg^{-1} \cdot h^{-1}$ dosage of ketamine and a 0.1 $mg \cdot kg^{-1} \cdot h^{-1}$ dosage of medetomidine. If an animal displayed a foot withdrawal reflex during anesthetic agent infusion, the infusion rate was increased by 30% until no reflex was observed. The femoral vein was cannulated for ^{11}C-flumazenil administration and the femoral artery for blood sampling. After cannulation, animals were positioned in the PET scanner. Animals were scanned in pairs using a high-resolution research tomograph comprising a double lutetium oxyorthosilicate–lutetium yttrium orthosilicate layer (CTI/Siemens) (*13*). First, for attenuation and scatter correction, a transmission scan was acquired using a 740-MBq 2-dimensional fan-collimated ^{137}Cs (662-keV) moving point source (*14*). Next, a dynamic emission scan was acquired immediately after the administration of approximately 25 MBq of ^{11}C-flumazenil to each animal. The exact radioactivity doses are displayed in Table 1. Data were [**Table 1**] acquired in list mode and rebinned into the following frame sequence: 6 × 10, 2 × 30, 3 × 60, 2 × 150, 2 × 300, and 1 × 600 s. After corrections for decay, dead time, scatter, and randoms, scans were reconstructed using an iterative 3-dimensional ordered-subsets weighted least-squares method (*15*). Point-source resolution varied across the field of view from approximately 2.3 to 3.2 mm in full width at half maximum in the transaxial direction and from 2.5 to 3.4 mm in full width at half maximum in the axial direction (*13*).

Each rat underwent 2 consecutive PET scans of 30 min. Before each scan, the tracer was mixed with a dose of isotopically unmodified (unlabeled) flumazenil (~4, 20, 100, or 400 μg) to achieve different receptor occupancies. The exact doses administered, which also depended on the amount of flumazenil in the tracer solution, were calculated and used for modeling (Table 1). Each rat was assigned 1 flumazenil dose—that is, both scans in 1 rat were obtained with the same amount of unlabeled flumazenil, enabling each rat to act as its own control for tariquidar treatment. Tariquidar, 3 ($n = 6$) or 15 ($n = 23$) $mg \cdot kg^{-1}$, was administered as an infusion over 10 min, starting 20 min before the second scan. The tariquidar doses were based on studies showing that 15 mg/kg results in complete inhibition of P-gp and 3 mg/kg is close to the median effective dose (*16*). The lower dose of 3 mg/kg can also be used in humans and could potentially allow for the translation of results between preclinical and clinical studies. Eight arterial blood samples of 0.1 mL were obtained in both kainate and control rats during each scan. The blood samples were immediately diluted with 0.5 mL of 0.42% NaF in water at 0°C to inhibit esterase activity, thus preventing flumazenil metabolism in the blood sample, and stored at −80°C until analysis.

Flumazenil Analysis in Blood Samples

Flumazenil concentrations in blood were analyzed using a previously published method comprising high-performance liquid chromatography coupled to tandem mass spectrometry (*17*). This analysis was performed in the same laboratory and with the same equipment (i.e., using identical conditions) as described in 2 previous reports (*17,18*). The limit of quantification was 0.5 $ng \cdot mL^{-1}$. Linear calibration curves were obtained in the range of 0.5–1,000 $ng \cdot mL^{-1}$.

Data Analysis

PET image data were analyzed using the freely available software package Amide 0.9 (*19*). An MRI-based rat brain atlas was used to define 5 regions of interest (ROIs) on the PET images. In short, the MRI atlas was aligned visually on a summation image of time frames from 30 to 270 s obtained from the tariquidar-treated rats. The following ROIs were selected: hippocampus, occipital cortex, parietal cortex, caudate putamen, and cerebellum (Fig. 1). These ROIs were then projected onto all frames from both [**Fig. 1**] scans, resulting in time–activity curves for each scan. The activity concentrations in the brain ROIs were converted to concentrations of flumazenil using:

TABLE 1
Data from First and Second PET Scans for Studied Rats

Characteristic	FMZ dose (μg)				All doses (μg)
	4	20	100	400	
No. of animals (*n*)*					
Controls	5	4	3	2	14
Kainate	5	6	2	2	15
Weight (g)					
Controls	279 ± 19	269 ± 10	285 ± 22	268 ± 4	276 ± 16
Kainate	293 ± 32	293 ± 51	281 ± 19	322 ± 21	295 ± 38
Scan radioactivity (MBq)					
First					
Controls	26 ± 3	23 ± 8	28 ± 3	19 ± 1	25 ± 5
Kainate	27 ± 6	27 ± 5	22 ± 3	23 ± 2	26 ± 5
Second					
Controls	23 ± 7	18 ± 2	24 ± 7	19 ± 3	21 ± 5
Kainate	23 ± 6	24 ± 9	28 ± 3	29 ± 5	25 ± 7
Flumazenil dose (μg)					
First scan					
Controls	3.5 ± 0.1	17 ± 1	84 ± 2	395 ± 81	NA
Kainate	3.5 ± 0.3	18 ± 1	79 ± 2	422 ± 15	NA
Second scan					
Controls	3.9 ± 0.2	18 ± 1	88 ± 3	424 ± 47	NA
Kainate	3.9 ± 0.2	19 ± 1	90 ± 3	459 ± 0	NA

*In addition to 29 rats displayed in table, 1 control rat died during surgery and 2 rats died as consequence of kainate treatment.
Values are displayed as average ± SD or *n*.
NA = not applicable.

$$C_{brT} = C_{brT,Act}/SA, \qquad \text{Eq. 1}$$

where SA ($Bq \cdot ng^{-1}$) is specific activity, C_{brT} ($ng \cdot mL^{-1}$) the unlabeled flumazenil concentration, and $C_{brT,Act}$ ($Bq \cdot mL^{-1}$) the measured radioactivity concentration in an ROI. SA was calculated from the injected amount of radioactivity (Act_{Dose} [Bq]) and the total dose of unlabeled flumazenil (FMZ_{Dose} [ng]) administered.

Data—that is, (unlabeled) flumazenil concentrations in blood and the 5 selected brain regions—were analyzed by mixed-effects modeling in NONMEM VI (GloboMax LLC). The subroutine ADVAN 6 and first-order conditional estimation with interaction were used throughout the modeling procedure. Model selection was based on the difference in the objective function values (OFV) between 2 nested models. The difference in OFV between 2 nested models is approximately χ^2 distributed. Hence, a difference of 3.84, 6.63, 7.88, and 10.83 points in the OFV is significant at a *P* value of 0.05, 0.01, 0.005, and 0.001, respectively (df = 1). A previous study (*18*) has verified that the full saturation approach used in the present study performs as well as the more established steady-state approach described by Lassen et al. (*20*), which requires at least 2 PET scans in each individual for separate estimates of B_{max} and K_D. A schematic representation of the pharmacokinetic model, consisting of 1 central plasma compartment, 1 peripheral tissue compartment, and 2 brain compartments, is shown in Figure 2. On administration into the central plasma compartment, flumazenil is distributed to peripheral tissue and brain-free compartments. In the brain, flumazenil can subsequently bind to $GABA_A$ receptors, which are represented by the second brain compartment. The brain concentration profile, as measured using PET, represents the total concentration in both brain compartments (C_{brT}). With this model, volumes of distribution in plasma, tissue, and brain compartments (V_1, V_2, and V_{br}); body clearance (CL); intercompartmental clearance (Q, Q_{in}, and Q_{out}); and specific binding to the benzodiazepine site on the $GABA_A$ receptors (B_{max}, k_{on}, and k_{off}) can all be estimated using the following equations:

$$\frac{d\left(C_{pl}\right)}{dt} \times V_1 = R_{inf} - (CL + Q + Q_{in}) \times C_{pl} + Q_{out} \times C_{brF} + Q \times C_{per}, \qquad \text{Eq. 2}$$

[**Fig. 2**]

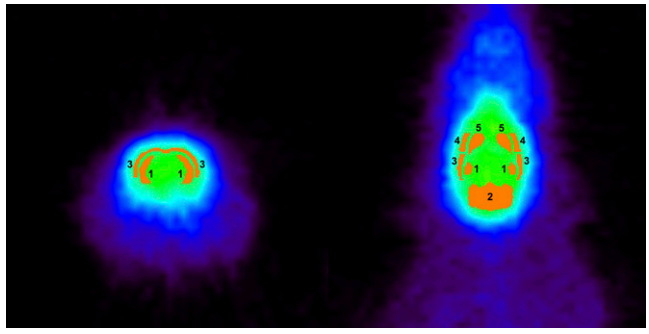

RGB

FIGURE 1. ROIs outlined on ^{11}C-flumazenil PET images: coronal (left) and axial (right) sections of rat brain. 1 = hippocampus; 2 = cerebellum; 3 = occipital cortex; 4 = parietal cortex; 5 = caudate putamen.

jnm104588-pm ■ 11/8/12

RGB

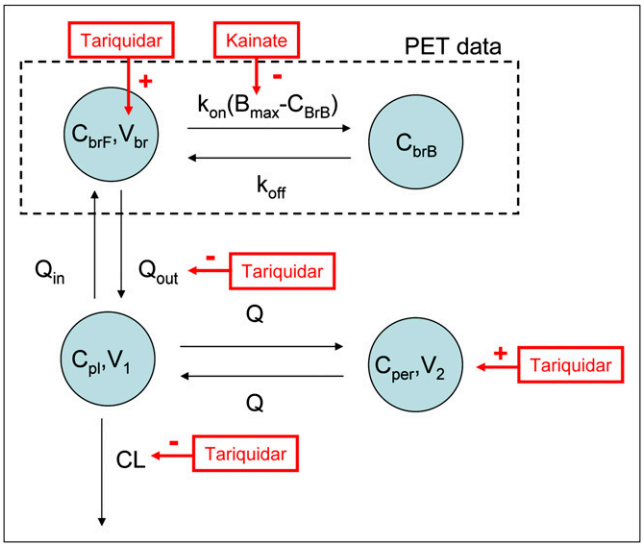

FIGURE 2. Pharmacokinetic model including effects of covariates: kainate and tariquidar treatment. CL is total-body clearance, Q is clearance between plasma and peripheral tissue, Q_{in} is clearance into brain, and Q_{out} is clearance out of brain. C_{pl} is flumazenil concentration in plasma and C_{per} in peripheral tissue. C_{brF} is free-plus-nonspecific as well as cerebral blood flumazenil concentration, and C_{brB} is $GABA_A$ receptor–bound flumazenil concentration, both in brain. Pharmacokinetic volumes of distribution are denoted by V_1 in plasma, V_2 in peripheral tissue, and V_{br} in brain. k_{on} is receptor association rate constant, k_{off} receptor dissociation rate constant, and B_{max} total concentration of receptors.

$$\frac{d\left(C_{per}\right)}{dt} \times V_2 = Q \times C_{pl} - Q \times C_{per}, \quad \text{Eq. 3}$$

$$\frac{d\left(C_{brF}\right)}{dt} \times V_{br} = Q_{in} \times C_{pl} - Q_{out} \times C_{brF} - k_{on} \times (B_{max} - C_{brB}) \times C_{brF} + k_{off} \times C_{brB}, \quad \text{Eq. 4}$$

$$\frac{d\left(C_{brB}\right)}{dt} = k_{on} \times (B_{max} - C_{brB}) \times C_{brF} - k_{off} \times C_{brB}, \quad \text{Eq. 5}$$

where $C_{pl} = \frac{A_{pl}}{V_1}$, $C_{per} = \frac{A_{per}}{V_2}$, and $C_{brF} = \frac{A_{brF}}{V_{br}}$.

R_{inf} is the zero-order administration rate ($ng \cdot min^{-1}$), calculated from the amount of injected flumazenil and the duration of the injection. CL is the total body clearance ($mL \cdot min^{-1}$), Q the intercompartmental clearance ($mL \cdot min^{-1}$) between plasma and peripheral tissue, Q_{in} the intercompartmental clearance ($mL \cdot min^{-1}$) across the blood–brain barrier into the brain, and Q_{out} the intercompartmental clearance ($mL \cdot min^{-1}$) across the blood–brain barrier out of the brain. C_{pl} is the flumazenil concentration ($ng \cdot mL^{-1}$) in plasma, and C_{per} is the concentration in peripheral tissue. C_{brF} is the free and nonspecifically bound flumazenil concentration ($ng \cdot mL^{-1}$) in the brain, and C_{brB} is the $GABA_A$ receptor–bound concentration ($ng \cdot mL^{-1}$) in the brain. A_{pl} is the amount of flumazenil (ng) in plasma, A_{per} (ng) the amount in peripheral tissue, and A_{brF} (ng) the free-plus-nonspecifically bound flumazenil in the brain. k_{on} is the receptor association rate constant ($mL \cdot min^{-1} \cdot ng^{-1}$), k_{off} the receptor dissociation rate constant (min^{-1}), and B_{max} ($ng \cdot ml^{-1}$) the total concentration of receptors. V_1, V_2, and V_{br} are pharmacokinetic volumes (mL) of distribution, which are used to scale amounts to concentrations.

K_D ($ng \cdot mL^{-1}$) is calculated as the ratio between k_{off} and k_{on}:

$$K_D = \frac{k_{off}}{k_{on}}. \quad \text{Eq. 6}$$

Residual errors were included for plasma and brain and were assumed to be proportional to the concentrations in plasma and brain, respectively.

Inclusion of interanimal variability, described by an exponential-variance model, was investigated for all structural model parameters:

$$\theta_i = \theta_{pop} \times \exp(\eta_i), \quad \text{Eq. 7}$$

where θ_i is the parameter in the ith animal, θ_{pop} the average population estimate of the parameter, and η_i the interanimal variability, which is assumed to be normally distributed around zero with an SD ω. Equation 7 provides a means to distinguish the parameter value for the ith animal from the population value predicted from the regression model. Interanimal variability was kept in the model if the OFV was decreased by more than 6.63 units, corresponding to a significant improvement of the model fit at the P value of less than 0.01.

Incorporation of kainate and tariquidar treatments as categoric covariates (Eq. 8) was investigated, whereas animal weight was considered as a continuous covariate for all model parameters (Eq. 9):

$$\theta_i = \theta_{pop} \times \exp(\eta_j) \times \theta_{covar}^{\text{COVARIATE (1 or 0)}}, \quad \text{Eq. 8}$$

$$\theta_i = \theta_{pop} \times WT/300 \times \theta_{covar}, \quad \text{Eq. 9}$$

where θ_{covar} describes the effect of weight, kainate treatment, or tariquidar treatment on the population parameter estimate θ_{pop}. In Equation 8, kainate and tariquidar treatment were assigned the value of 1, whereas no treatment was assigned the value of 0. The θ_{covar} estimate therefore represents the fractional change between treated and untreated groups. In Equation 9, WT is the animal weight in grams, and the effect of the covariate was described relative to the typical animal weight of 300 g. Final equations for all model parameters are given in Table 2. [**Table 2**]

A stepwise forward-inclusion and backward-elimination strategy was used to develop the covariate model. In the forward-inclusion step, a covariate was included if it resulted in an OFV reduction of more than 3.83 units ($P < 0.05$). In the backward-elimination step, the covariate was kept in the model only if the OFV increased by more than 6.68 ($P < 0.01$) units when it was excluded.

In addition to OFV reductions, parameter uncertainty and different types of goodness-of-fit plots were used to assess the model performance throughout the modeling procedure. The software Xpose 4 implemented in R 2.7.1 (The R foundation for Statistical Computing) was used for visual inspection of model performance (*21*). All brain areas were included in the analysis—that is, each region was assigned a region-specific B_{max} parameter. The model was also run separately for each brain region to study whether regional differences existed in any model parameters other than B_{max}. The final model was then rerun separately using data from animals administered only 3 or 15 $mg \cdot kg^{-1}$ of tariquidar and separately using data from animals studied at 2 and 7 d after kainate treatment to investigate further the effect of tariquidar

TABLE 2
Final Parameter Equations Describing Pharmacokinetic Model

Model	Equation
Plasma	$V_1 = \theta_1 \times \exp(\eta_1)$
	$V_2 = \theta_2 \times \theta_3^{\text{TARIQUIDAR}}$
	$CL = \theta_4 \theta_5^{\text{TARIQUIDAR}} \times \exp(\eta_2)$
	$Q = \theta_6$
Brain	$Q_{in} = \theta_7 \cdot \exp(\eta_3)$
	$Q_{out} = Q_{in} \theta_8^{(1 - \text{TARIQUIDAR})} \times \exp(\eta_4)$
	$V_{Br} = \theta_9 \theta_{10}^{\text{TARIQUIDAR}} \exp(\eta_5)$
	$k_{off} = \theta_{11} \cdot \exp(\eta_6)$
	$K_D = \theta_{12} \cdot \exp(\eta_7)$
	$B_{max\ hippocampus} = \theta_{13} \cdot \theta_{18}^{\text{KAINATE}}$
	$B_{max\ cerebellum} = \theta_{14} \cdot \theta_{18}^{\text{KAINATE}}$
	$B_{max\ caudate\ putamen} = \theta_{15} \cdot \theta_{18}^{\text{KAINATE}}$
	$B_{max\ occipital\ cortex} = \theta_{16} \cdot \theta_{18}^{\text{KAINATE}}$
	$B_{max\ parietal\ cortex} = \theta_{17} \cdot \theta_{18}^{\text{KAINATE}}$

Covariates KAINATE and TARIQUIDAR were set to 1 for treated animals and to 0 for nontreated animals. All θ and η were estimated in optimization of model. Interanimal variability, described by exponential variance model—that is, exp(η)—was investigated for all structural model parameters but kept in model only if model was significantly improved by inclusion.

dose and time after kainate treatment. To investigate whether the effect of tariquidar was different in kainate-treated and control animals, the model was also fitted separately to these 2 groups. Finally, to investigate whether B_{max} estimates were affected by P-gp function, pre- and posttariquidar scans were analyzed separately, and B_{max} estimates were compared. Parameter estimates are reported as average ± SE.

RESULTS

^{11}C-flumazenil pharmacokinetics in plasma and 5 different brain regions were studied in control and kainate-treated rats, a model for temporal lobe epilepsy, before and after tariquidar administration. Flumazenil concentrations over time in the hippocampus of control and kainate-treated rats are shown in Figure 3, displayed for the groups dosed with the lowest cold flumazenil dose, because control and kainate rats received the same amount of flumazenil in both scans (3.5 μg in scan 1 and 3.9 μg in scan 2; Table 1). In all dose groups, flumazenil concentrations were lower in kainate-treated than in control rats.

[**Fig. 3**]

Receptor Density and Affinity

The estimates of all model parameters are shown in Table 3, and goodness-of-fit plots are shown in Figure 4. K_D was estimated as 5.9 ± 0.9 ng·mL^{-1} and was not affected by any of the covariates studied. The time–activity profiles showed that flumazenil binding was most prominent in the hippocampus, whereas the cerebellum displayed the lowest binding. The hippocampus B_{max} was estimated as 44 ± 2 and cerebellum B_{max} as 33 ± 2 ng·mL^{-1}. Receptor densities in the occipital cortex, parietal cortex, and caudate putamen were intermediate, compared with those in the hippocampus and cerebellum, and are shown in Table 3. In line with the lower flumazenil brain concentrations in kainate-treated animals, kainate treatment was found to be a significant covariate for B_{max}, producing a 12% decrease in the number of $GABA_A$ receptors available for flumazenil binding. Tariquidar treatment was not found to be a significant covariate for B_{max}, and B_{max} estimates were similar when data from pre- and posttariquidar scans were analyzed separately (Table 4).

[**Table 3**]
[**Fig. 4**]

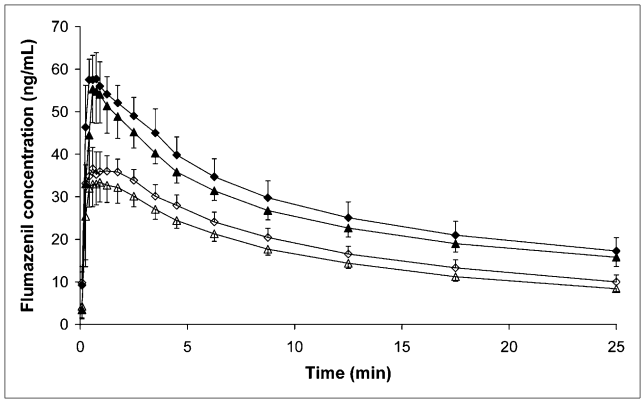

FIGURE 3. Flumazenil concentrations in hippocampus in control (diamonds) and kainate (triangles) animals that were dosed with approximately 4 μg of flumazenil (3.5 μg in scan 1 and 3.9 μg in scan 2). Open and closed symbols represent scans before and after tariquidar treatment. Error bars indicate SD. Flumazenil concentrations were lower in kainate-treated rats than in controls, both before and after tariquidar treatment.

Regional Differences

The final model was also fitted to each region separately to investigate whether the effect of kainate treatment was of the same magnitude in different regions or whether there were differences in parameter values between regions. A small regional difference in the kainate-induced reduction in B_{max} was found (Table 4). B_{max} decreased by 12% in the cerebellum, whereas the effect of kainate treatment was larger in other regions, producing a decrease of 15% in the hippocampus, 20% in the occipital cortex, 26% in the parietal cortex, and 16% in the caudate putamen. To investigate this regional difference further, the model was fitted with region-specific covariates for the kainate effect, but this led to an OFV reduction of less than 6.64 units, suggesting that the model as a whole did not improve. There were no differences in any of the other model parameters when regions were fitted separately (Table 4).

Effect of Tariquidar and Kainate Treatment on Flumazenil Pharmacokinetics

The effect of tariquidar treatment on transport across the blood–brain barrier was best described by a model in which

TABLE 3
Parameter Value Estimates for All Rats Analyzed Simultaneously and Specifically for Control and Kainate-Treated Groups

Fixed effects	All	Controls	Kainate-treated group
B_{max} (ng·mL^{-1})			
Hippocampus	44 ± 2	43 ± 2	39 ± 2
Cerebellum	33 ± 2	32 ± 2	29 ± 2
Caudate putamen	40 ± 2	40 ± 2	35 ± 2
Occipital cortex	40 ± 2	38 ± 2	34 ± 2
Parietal cortex	39 ± 2	39 ± 2	34 ± 2
K_D (ng·mL^{-1})	5.9 ± 0.9	6.3 ± 1.1	5.6 ± 0.8
V_1 (mL)	51 ± 4	63 ± 7	46 ± 5
V_2 (mL)	122 ± 6	143 ± 9	115 ± 10
CL (mL· min^{-1})	37 ± 5	66 ± 10	31 ± 5
Q (mL· min^{-1})	19 ± 1	20 ± 1	19 ± 2
V_{br} (mL)	8.5 ± 2.7	5.2 ± 2.5	7.2 ± 3.3
Q_{in}/Q_{out} (mL· min^{-1})	37 ± 14	61 ± 21	23 ± 13
k_{off} (min^{-1})	0.23 ± 0.06	0.16 ± 0.02	0.42 ± 0.17
Covariates			
Kainate (B_{max})	0.88 ± 0.05	NA	NA
Tariquidar	0.84 ± 0.05	0.74 ± 0.06	0.84 ± 0.05
CL			
V_2	1.23 ± 0.06	1.14 ± 0.05	1.23 ± 0.10
Q_{out}	1.73 ± 0.06	1.75 ± 0.07	1.73 ± 0.10
V_{br}	1.24 ± 0.10	1.48 ± 0.14	1.26 ± 0.12
Interanimal variability (η-shrinkage)			
V_1	0.05 ± 0.02 (23)	0.02 ± 0.01 (28)	0.04 ± 0.02 (17)
CL	0.15 ± 0.05 (16)	0.03 ± 0.02 (17)	0.13 ± 0.05 (1)
Q_{in}	1.04 ± 0.38 (15)	<0.01	2.48 ± 0.75 (5)
Q_{out}	0.03 ± 0.01 (24)	0.05 ± 0.02 (42)	0.05 ± 0.03 (12)
V_{br}	0.54 ± 0.22 (25)	0.06 ± 0.03 (19)	1.25 ± 0.51 (12)
k_{off}	0.77 ± 0.57 (37)	<0.01	1.29 ± 0.77 (32)
K_D	0.16 ± 0.06 (34)	0.08 ± 0.04 (46)	0.21 ± 0.09 (19)
Residual errors			
Blood	0.46 ± 0.03	0.37 ± 0.03	0.54 ± 0.05
Brain	0.12 ± 0.01	0.07 ± 0.004	0.14 ± 0.02

Values are presented as average ± SE. Data in parentheses are percentages. Covariates are expressed as fractional change.
NA = not applicable.

Q_{in} equals Q_{out} after tariquidar treatment. Q_{out} decreased by 73% after tariquidar treatment. The post hoc individual estimates showed that kainate-treated rats had a somewhat lower Q_{in} than control rats. To study this observation further, the model was fitted to control and kainate rats separately and, in line with the post hoc estimates, Q_{in} was estimated as 61 ± 21 mL·min^{-1} in control rats and 23 ± 13 mL·min^{-1} in kainate-treated rats. In addition, the separation of control and kainate-treated rats showed that although interanimal variability for Q_{in} was absent in the control group, Q_{in} was the parameter with the highest interanimal variability in the kainate-treated group (Table 3). Adding a covariate on Q_{in} for kainate treatment resulted in a drop in OFV of only 2 units—that is, a nonsignificant improvement of the model. Separate analysis showed that the tariquidar effect on Q_{out} was the same in control and kainate-treated rats (Table 3). Tariquidar treatment also increased V_{br} by 24% and affected plasma pharmacokinetics: CL decreased by 16% and V_2 increased by 23%, as shown in Table 3.

Six animals were administered a 3 mg·kg^{-1} dose of tariquidar, whereas all others received 15 mg·kg^{-1}. The model was fitted to these 2 groups separately, and although the sparse data in the 3 mg·kg^{-1} group did not allow for an estimation of SEs (in NONMEM), there was no difference between these 2 groups (data not shown). In addition, the post hoc model parameter estimates did not suggest any difference between animals treated with 3 and 15 mg·kg^{-1} doses of tariquidar. The model was also fitted excluding data from the 3 animals that were scanned 2 d after kainate treatment, but this did not change parameter estimates. Post hoc estimates obtained with the final model and all data showed that animals scanned 2 d after kainate treatment tended to have a somewhat reduced CL of 24 mL·min^{-1}, compared with 38 mL·min^{-1} in animals scanned 7 d after kainate treatment.

Interanimal variation was observed for most of the parameters (Table 3). The separate model fits in control and kainate-treated animals showed that, in general, interanimal variability was much larger in the kainate-treated group.

jnm104588-pm ■ 11/8/12

RGB

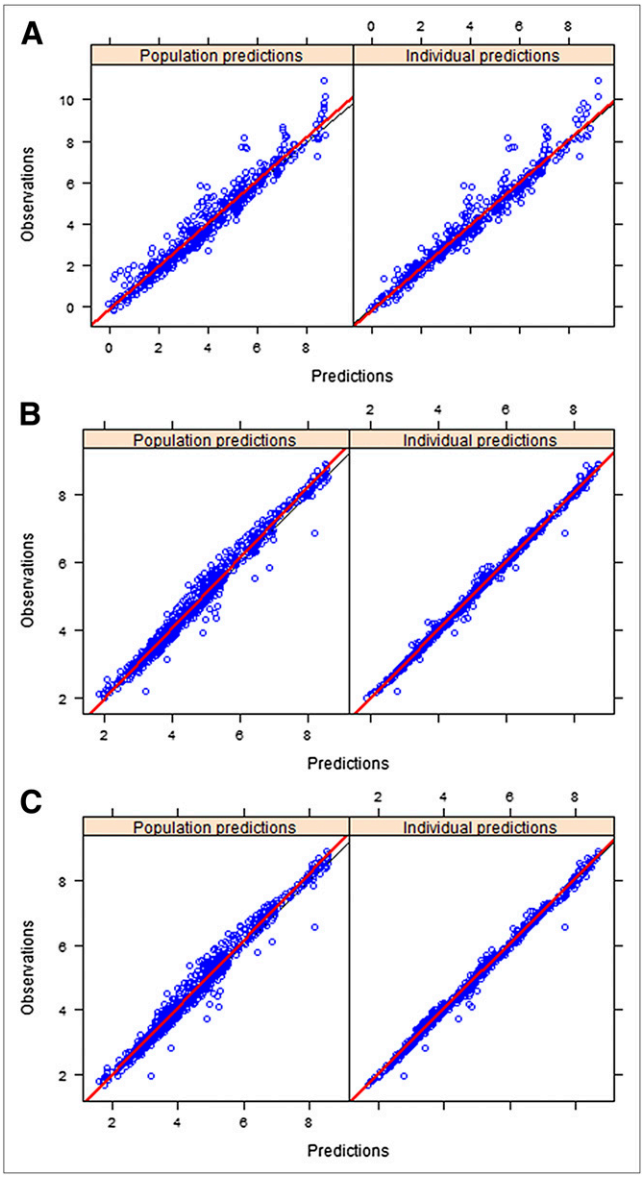

FIGURE 4. Observed (*y*-axis) vs. predicted (*x*-axis) concentrations are shown in plasma (A), hippocampus (B), and cerebellum (C) using final model. All dots represent individual data points, thin black lines are identity lines, and red lines show average observation. Model describes ^{11}C-flumazenil concentrations, and both population and individual predictions are randomly distributed around line of identity. Inclusion of interanimal variation improved model because spread of residuals around line of identity was smaller (=improved fit) in plots showing individual predictions (right) than in those showing population predictions (left).

DISCUSSION

The objective of this study was to investigate if flumazenil blood–brain barrier transport and binding to the benzodiazepine site on the $GABA_A$ receptors is altered in kainate-treated rats, compared with controls, and whether changes in P-gp function may confound interpretation of ^{11}C-flumazenil PET. Results suggested that receptor density, B_{max}, was lower in kainate-treated animals than in controls. This result is in line with previous preclinical and clinical studies using ^{11}C-flumazenil (*17,22*) and suggests a reduction in $GABA_A$ receptor binding capacity in the epileptic brain, compared with the naïve brain. A previous study in kindled rats, another rat model for temporal lobe epilepsy (*23,24*), showed that B_{max} was reduced by 36%, compared with controls (*17*). In the present study, a reduction of 12% was found. It is likely that B_{max} was reduced more in the kindled rats, because they were scanned between 14 and 28 d after they had experienced 6 stage V seizures. Thus, the reduction in B_{max} may be progressive, and it would be of interest to investigate B_{max} as a function of time after status epilepticus. The present study showed that B_{max} is different in different brain regions and also suggested that the decrease in B_{max} after kainate treatment might be region-dependent, with a lower reduction in the cerebellum, a brain region that is not involved in generating epileptic activity. The model assumes that flumazenil transport into the brain, as well as the association and dissociation rate with the receptors, is similar in all brain regions. This assumption was supported by fitting of the model to each region separately, where no other regional differences in parameter estimates were shown. Hence, the decreased efficacy of GABAergic drugs observed in epilepsy is most likely caused by a lower number of $GABA_A$ receptors rather than an alteration in binding affinity (K_D) to the receptors.

The estimated B_{max} for the hippocampus of 44 ng·mL^{-1} (corresponding to 146 pmol mg^{-1} of brain tissue, assuming that 1 cm^3 of brain tissue contains 100 mg of protein) is similar to a previously reported B_{max} estimate of 45 ng·mL^{-1} using the same PET protocol and pharmacokinetic model (*18*). Liefaard et al. reported somewhat lower B_{max} estimates of 25 and 19 ng·mL^{-1} in control and kindled rats, respectively (*17,25*). Their findings may be due to different ROI definitions (because Liefaard et al. did not coregister PET images with an MRI-based brain template) or use of different rat strains (Wistar vs. Sprague–Dawley) and experimental set-up. The B_{max} estimates were also in line with previously published in vitro estimates assuming that 1 cm^3 of brain tissue contains 100 mg of protein: 4.4 ng·mL^{-1} in living rat cortex slices (*26*), 3.3 ng·mL^{-1} in rat cortex homogenates (*27*), and 54.5 ng·mL^{-1} in rat brain homogenates (*28*). The K_D estimate, 5.9 ± 0.9 ng·mL^{-1}, obtained in the present study is also in line with previously published studies (*17,18,25–28*). On the basis of time–activity data obtained in a previous study when ^{11}C-flumazenil was administered without the addition of unlabeled flumazenil (*18*), the doses used in the present study resulted in approximate occupancy levels of 30%–40% for 4-μg, 60%–70% for 20-μg, 70%–80% for 100-μg, and around 90% for 400-μg dose groups.

Tariquidar treatment decreased the Q_{out} of flumazenil by 73%, confirming initial in vivo reports that flumazenil is a P-gp substrate in rodents (*7*). Tariquidar also increased V_{br} by 24%. Increased V_{br} after tariquidar treatment has

TABLE 4
Parameter Estimates for Brain Model When Different Brain Regions and Scans Were Analyzed Separately

Fixed effects	All regions	Hippocampus	Cerebellum	Caudate putamen	Occipital cortex	Parietal cortex	Scan 1 (before tariquidar)	Scan 2 (after tariquidar)
B_{max} (ng·mL^{-1})								
Hippocampus	44 ± 2	45 ± 2	NA	NA	NA	NA	43 ± 6	46 ± 2
Cerebellum	33 ± 2	NA	32 ± 3	NA	NA	NA	32 ± 2	35 ± 2
Caudate putamen	40 ± 2	NA	NA	40 ± 2	NA	NA	39 ± 2	43 ± 2
Occipital cortex	40 ± 2	NA	NA	NA	45 ± 3	NA	39 ± 2	40 ± 2
Parietal cortex	39 ± 2	NA	NA	NA	NA	45 ± 2	39 ± 2	41 ± 2
K_D (ng·mL^{-1})	5.9 ± 0.9	5.6 ± 0.7	5.1 ± 0.8	5.7 ± 0.7	5.1 ± 0.7	5.1 ± 0.6	5.2 ± 0.7	5.1 ± 0.5
V_{br} (mL)	8.5 ± 2.7	11.6 ± 2.6	9.7 ± 2.0	11.6 ± 3.1	15.2 ± 3.2	12.6 ± 2.8	5.1 ± 5.5	10.9 ± 2.7
Q_{in}/Q_{out} (mL·min-1)	37 ± 14	69 ± 19	68 ± 17	64 ± 18	72 ± 18	63 ± 17	26 ± 30	44 ± 14
Covariates								
Kainate (B_{max})	0.88 ± 0.05	0.85 ± 0.05	0.88 ± 0.08	0.84 ± 0.06	0.80 ± 0.06	0.74 ± 0.05	0.89 ± 0.06	0.84 ± 0.04
Tariquidar								
Q_{out}	1.73 ± 0.06	1.68 ± 0.03	1.67 ± 0.03	1.71 ± 0.03	1.65 ± 0.03	1.70 ± 0.03	NA	NA
V_{br}	1.24 ± 0.10	1.18 ± 0.11	1.31 ± 0.14	1.20 ± 0.13	1.20 ± 0.10	1.27 ± 0.11	NA	NA

Values are presented as average ± SE.
NA = not applicable.

also been reported in other pharmacokinetic studies for both flumazenil and other P-gp substrates (*17,29–31*). The V_{br} estimate can be compared with the physical brain volume, which, for a rat, is about 2 g (i.e., 2 mL). If the volume estimate is larger than the actual brain volume, it means that the substance is unevenly distributed in hydrophilic and lipophilic parts of the brain (*32,33*). The increase in V_{br} suggests that tariquidar selectively enhances uptake of flumazenil in deeper (lipophilic) parts of the brain.

Both clinical and preclinical studies have reported small, but significant, regional differences in increasing concentrations of the P-gp substrate radiotracer (*R*)-^{11}C-verapamil after P-gp inhibition (*16,34,35*). In contrast, effects of tariquidar on Q_{out} and V_{br} were similar in all brain regions studied in the present study (Table 4). Verapamil, however, is a much stronger P-gp substrate than flumazenil, showing a more than 1,000% increase in brain concentrations after P-gp inhibition with a 15 mg·kg^{-1} dose of tariquidar (*29,36*), and it is possible that regional differences between flumazenil brain concentrations at baseline and after P-gp inhibition are too small to be detected. The present study also showed that the effects of tariquidar were similar for kainate-treated animals and controls (Table 2). Effects of tariquidar on the plasma parameters CL and V_2 are more likely due to P-gp expression in other tissues than to the blood–brain barrier, restricting flumazenil peripheral distribution.

As different studies have reported maximum P-gp expression at different time points after kainate-induced status epilepticus (*29,37,38*), 3 animals were scanned 2 rather than 7 d after kainate treatment. In addition, it has also been proposed that differences in P-gp functionality are clearer after submaximum P-gp inhibition using 3 mg·kg^{-1} of tariquidar rather than using a 15 mg·kg^{-1} dose that completely inhibits P-gp (*34*). Thus, time after kainate treatment (2 or 7 d) and tariquidar dose (3 or 15 mg·kg^{-1}) were initially included as possible covariates, but these did not improve the model. Further, post hoc individual estimates were investigated, and this approach did not reveal any trend between time after kainate treatment or tariquidar dose and any of the model parameters, except that CL was somewhat decreased in animals scanned at 2 d after kainate treatment, compared with animals scanned at 7 d.

At the time of the PET study, kainate will be completely eliminated from the animals and will therefore not interfere with the pharmacokinetics of flumazenil. Anesthesia, on the other hand, may influence the brain pharmacokinetics of flumazenil. The anesthetic drugs used in the present study (ketamine and medetomidine) were chosen because they, in contrast to isoflurane, do not directly interfere with the $GABA_A$ receptor complex (*39,40*). Nevertheless, translation of preclinical results performed under anesthesia to the clinical situation should always be done with caution.

In the clinic, ^{11}C-flumazenil is used to assess GABAergic function in epilepsy and to determine focus localization

before resective surgery. Studies have shown that P-gp is upregulated in epilepsy (*8,9,41,42*), and hence ^{11}C-flumazenil brain concentrations might be lowered because of both impaired GABAergic function and increased P-gp mediated efflux out of the brain. The present study showed that effects of tariquidar treatment, which induces an alteration in P-gp function, were similar in kainate-treated animals and controls. Even if P-gp is upregulated more in human epilepsy, effects on cerebral ^{11}C-flumazenil concentrations are likely to be small, because complete P-gp inhibition in the present study resulted in only a 73% decrease in Q_{out}, which was partly counteracted by an increase in V_{br}. To investigate further the risk of erroneous interpretation with respect to GABAergic function in epilepsy, the model was run separately for pre- and posttariquidar scans. B_{max} estimates were only slightly increased for posttariquidar, compared with pretariquidar, data (Table 4), suggesting that B_{max} estimates are not affected much by alterations in P-gp function.

The present study also demonstrated that there was much more interanimal variability in the disease model (kainate group) than in control rats (Table 3). The use of a population approach, which is not standard in the PET community, is well suited to handle this type of data, because it allows for the estimation of both structural model parameters and variability within the population.

CONCLUSION

The present study showed that B_{max} for the $GABA_A$ ligand flumazenil was reduced in kainate-treated rats, compared with controls. B_{max}, and possibly the kainate-induced reduction in B_{max}, were region-specific, with the hippocampus showing the highest B_{max} and the cerebellum the lowest, as well as the smallest decrease after kainate treatment. P-gp inhibition reduced Q_{out} by 73%, suggesting that flumazenil is a weak P-gp substrate in rats. It is unlikely, however, that B_{max} estimates are affected by alterations in P-gp functionality.

ACKNOWLEDGMENTS

We thank Maarten Schenke, Inge de Greeuw, Marc Huisman, and Carla Molthoff for assistance with animal surgery and PET scanning. We are also grateful to the radiochemists of the Department of Nuclear Medicine and PET Research at the VU Medical Center in Amsterdam for the syntheses of ^{11}C-flumazenil. This work was supported by the EU 7th framework programme EURIPIDES (FP7/2007-2013 under grant agreement 201380). No other potential conflict of interest relevant to this article was reported.

REFERENCES

1. Jefferys JG. Basic mechanisms of focal epilepsies. *Exp Physiol.* 1990;75:127–162.
2. McCormick DA, Contreras D. On the cellular and network bases of epileptic seizures. *Annu Rev Physiol.* 2001;63:815–846.
3. Rogawski MA, Löscher W. The neurobiology of antiepileptic drugs. *Nat Rev Neurosci.* 2004;5:553–564.
4. Meldrum BS, Rogawski MA. Molecular targets for antiepileptic drug development. *Neurotherapeutics.* 2007;4:18–61.
5. Remy S, Beck H. Molecular and cellular mechanisms of pharmacoresistance in epilepsy. *Brain.* 2006;129:18–35.
6. Schmidt D, Loscher W. New developments in antiepileptic drug resistance: an integrative view. *Epilepsy Curr.* 2009;9:47–52.
7. Ishiwata K, Kawamura K, Yanai K, Hendrikse NH. In vivo evaluation of P-glycoprotein modulation of 8 PET radioligands used clinically. *J Nucl Med.* 2007;48:81–87.
8. Löscher W, Potschka H. Role of drug efflux transporters in the brain for drug disposition and treatment of brain diseases. *Prog Neurobiol.* 2005;76:22–76.
9. Sisodiya SM, Lin WR, Harding BN, Squier MV, Thom M. Drug resistance in epilepsy: expression of drug resistance proteins in common causes of refractory epilepsy. *Brain.* 2002;125:22–31.
10. Hellier JL, Patrylo PR, Buckmaster PS, Dudek FE. Recurrent spontaneous motor seizures after repeated low-dose systemic treatment with kainate: assessment of a rat model of temporal lobe epilepsy. *Epilepsy Res.* 1998;31:73–84.
11. Racine R, Okujava V, Chipashvili S. Modification of seizure activity by electrical stimulation. 3. Mechanisms. *Electroencephalogr Clin Neurophysiol.* 1972;32:295–299.
12. Maziere M, Hantraye P, Prenant C, Sastre J, Comar D. Synthesis of ethyl 8-fluoro-5,6-dihydro-5-[^{11}C]methyl-6-oxo-4H-imidazo [1,5-a] [1,4]benzodiazepine-3-carboxylate (RO 15.1788-^{11}C): a specific radioligand for the in vivo study of central benzodiazepine receptors by positron emission tomography. *Int J Appl Radiat Isot.* 1984;35:973–976.
13. de Jong HW, van Velden FH, Kloet RW, Buijs FL, Boellaard R, Lammertsma AA. Performance evaluation of the ECAT HRRT: an LSO-LYSO double layer high resolution, high sensitivity scanner. *Phys Med Biol.* 2007;52:1505–1526.
14. van Velden FH, Kloet RW, van Berckel BN, et al. Impact of attenuation correction strategies on the quantification of High Resolution Research Tomograph PET studies. *Phys Med Biol.* 2008;53:99–118.
15. van Velden FH, Kloet RW, van Berckel BN, et al. HRRT versus HR+ human brain PET studies: an interscanner test-retest study. *J Nucl Med.* 2009;50:693–702.
16. Kuntner C, Bankstahl JP, Bankstahl M, et al. Dose-response assessment of tariquidar and elacridar and regional quantification of P-glycoprotein inhibition at the rat blood-brain barrier using (R)-[(11)C]verapamil PET. *Eur J Nucl Med Mol Imaging.* 2010;37:942–953.
17. Liefaard LC, Ploeger BA, Molthoff CF, et al. Changes in GABAA receptor properties in amygdala kindled animals: in vivo studies using [^{11}C]flumazenil and positron emission tomography. *Epilepsia.* 2009;50:88–98.
18. Syvänen S, de Lange EC, Tagawa Y, et al. Simultaneous in vivo measurements of receptor density and affinity using [^{11}C]flumazenil and positron emission tomography: comparison of full saturation and steady state methods. *Neuroimage.* 2011;57:928–937.
19. Loening AM, Gambhir SS. AMIDE: a free software tool for multimodality medical image analysis. *Mol Imaging.* 2003;2:131–137.
20. Lassen NA, Bartenstein PA, Lammertsma AA, et al. Benzodiazepine receptor quantification in vivo in humans using [^{11}C]flumazenil and PET: application of the steady-state principle. *J Cereb Blood Flow Metab.* 1995;15:152–165.
21. Jonsson EN, Karlsson MO. Xpose - an S-PLUS based population pharmacokinetic/pharmacodynamic model building aid for NONMEM. *Comput Methods Programs Biomed.* 1999;58:51–64.
22. Lamusuo S, Pitkanen A, Jutila L, et al. [11 C]Flumazenil binding in the medial temporal lobe in patients with temporal lobe epilepsy: correlation with hippocampal MR volumetry, T2 relaxometry, and neuropathology. *Neurology.* 2000;54:2252–2260.
23. Morimoto K, Fahnestock M, Racine RJ. Kindling and status epilepticus models of epilepsy: rewiring the brain. *Prog Neurobiol.* 2004;73:1–60.
24. Löscher W. Animal models of epilepsy for the development of antiepileptogenic and disease-modifying drugs: a comparison of the pharmacology of kindling and post-status epilepticus models of temporal lobe epilepsy. *Epilepsy Res.* 2002;50:105–123.
25. Liefaard LC, Ploeger BA, Molthoff CF, et al. Population pharmacokinetic analysis for simultaneous determination of B (max) and K (D) in vivo by positron emission tomography. *Mol Imaging Biol.* 2005;7:411–421.
26. Murata T, Matsumura K, Onoe H, et al. Receptor imaging technique with ^{11}C-labeled receptor ligands in living brain slices: its application to time-resolved imaging and saturation analysis of benzodiazepine receptor using [^{11}C]Ro15-1788. *Neurosci Res.* 1996;25:145–154.
27. Visser SA, Wolters FL, Gubbens-Stibbe JM, et al. Mechanism-based pharmacokinetic/pharmacodynamic modeling of the electroencephalogram effects of GA-

BAA receptor modulators: in vitro-in vivo correlations. *J Pharmacol Exp Ther.* 2003;304:88–101.
28. Mandema JW, Sansom LN, Dios-Vieitez MC, Hollander-Jansen M, Danhof M. Pharmacokinetic-pharmacodynamic modeling of the electroencephalographic effects of benzodiazepines: correlation with receptor binding and anticonvulsant activity. *J Pharmacol Exp Ther.* 1991;257:472–478.
29. Syvänen S, Luurtsema G, Molthoff CF, et al. (R)-[^{11}C]verapamil PET studies to assess changes in P-glycoprotein expression and functionality in rat blood-brain barrier after exposure to kainate-induced status epilepticus. *BMC Med Imaging.* 2011;11:1–16.
30. Clinckers R, Smolders I, Michotte Y, et al. Impact of efflux transporters and of seizures on the pharmacokinetics of oxcarbazepine metabolite in the rat brain. *Br J Pharmacol.* 2008;155:1127–1138.
31. Syvänen S, Schenke M, van den Berg DJ, Voskuyl RA, de Lange EC. Alteration in P-glycoprotein functionality affects intrabrain distribution of quinidine more than brain entry-a study in rats subjected to status epilepticus by kainate. *AAPS J.* 2012;14:87–96.
32. Hammarlund-Udenaes M, Friden M, Syvänen S, Gupta A. On the rate and extent of drug delivery to the brain. *Pharm Res.* 2008;25:1737–1750.
33. Syvänen S, Xie R, Sahin S, Hammarlund-Udenaes M. Pharmacokinetic consequences of active drug efflux at the blood-brain barrier. *Pharm Res.* 2006;23:705–717.
34. Bankstahl JP, Bankstahl M, Kuntner C, et al. A novel positron emission tomography imaging protocol identifies seizure-induced regional overactivity of P-glycoprotein at the blood-brain barrier. *J Neurosci.* 2011;31:8803–8811.
35. Bauer M, Karch R, Neumann F, et al. Assessment of regional differences in tariquidar-induced P-glycoprotein modulation at the human blood-brain barrier. *J Cereb Blood Flow Metab.* 2010;30:510–515.
36. Bankstahl JP, Kuntner C, Abrahim A, et al. Tariquidar-induced P-glycoprotein inhibition at the rat blood-brain barrier studied with (R)-^{11}C-verapamil and PET. *J Nucl Med.* 2008;49:1328–1335.
37. Seegers U, Potschka H, Loscher W. Transient increase of P-glycoprotein expression in endothelium and parenchyma of limbic brain regions in the kainate model of temporal lobe epilepsy. *Epilepsy Res.* 2002;51:257–268.
38. Zhang L, Ong WY, Lee T. Induction of P-glycoprotein expression in astrocytes following intracerebroventricular kainate injections. *Exp Brain Res.* 1999;126:509–516.
39. Albertson TE, Walby WF, Joy RM. Modification of GABA-mediated inhibition by various injectable anesthetics. *Anesthesiology.* 1992;77:488–499.
40. Buggy DJ, Nicol B, Rowbotham DJ, Lambert DG. Effects of intravenous anesthetic agents on glutamate release: a role for GABAA receptor-mediated inhibition. *Anesthesiology.* 2000;92:1067–1073.
41. Tishler DM, Weinberg KI, Hinton DR, Barbaro N, Annett GM, Raffel C. MDR1 gene expression in brain of patients with medically intractable epilepsy. *Epilepsia.* 1995;36:1–6.
42. Dombrowski SM, Desai SY, Marroni M, et al. Overexpression of multiple drug resistance genes in endothelial cells from patients with refractory epilepsy. *Epilepsia.* 2001;42:1501–1506.

jnm104588-pm ■ 11/8/12